The Cryosphere Discuss., 5, 3517–3539, 2011
www.the-cryosphere-discuss.net/5/3517/2011/
doi:10.5194/tcd-5-3517-2011

The Cryosphere Discussions

Melting of Northern Greenland during the last interglacial

A. Born[1,2] **and K. H. Nisancioglu**[3,4]

[1]Climate and Environmental Physics, Physics Institute, University of Bern, Bern, Switzerland
[2]Oeschger Centre for Climate Change Research, Bern, Switzerland
[3]Bjerknes Centre for Climate Research, Bergen, Norway
[4]UNI Research, Bergen, Norway

Received: 21 November 2011 – Accepted: 10 December 2011
– Published: 21 December 2011

Correspondence to: A. Born (born@climate.unibe.ch)

Published by Copernicus Publications on behalf of the European Geosciences Union.

Abstract

The Greenland ice sheet (GrIS) is losing mass at an increasing rate, making it the primary contributor to global eustatic sea level rise. Large melting areas and rapid thinning at its margins has raised concerns about its stability. However, it is conceivable that these observations represent the transient adjustment of the fastest reacting parts of the ice sheet, masking slower processes that dominate the long term fate of the GrIS and its contribution to sea level rise.

Studies of the geological past provide valuable information on the long term response of the GrIS to warm periods. We simulate the GrIS during the Eemian interglacial, a period 126 000 yr before present (126 ka) with Arctic temperatures comparable to projections for the end of this century. The northeastern part of the GrIS is unstable and retreats significantly, despite moderate melt rates. Unlike the south and west, strong melting in the northeast is not compensated by high accumulation, or fast ice flow. The analogy with the present warming suggests that in coming decades, positive feedbacks could increase the rate of mass loss of the northeastern GrIS, exceeding the currently observed melting in the south.

1 Introduction

The last interglacial, the Eemian, is considered the warmest period of the past 150 thousand years (Jansen et al., 2007). Evidence from fossil coral reefs suggest a sea level high stand of 4 to 8 m (Overpeck et al., 2006; Kopp et al., 2009) and temperatures on and around Greenland 4–5 °C higher than today (CAPE members, 2006; Otto-Bliesner et al., 2006). The warming was caused by a change in seasonal insolation (Loutre et al., 2004), while greenhouse gas concentrations were comparable to preindustrial values (Petit et al., 1999). Nevertheless, the reconstructed warming of the Arctic during the Eemian is similar to the projected 2.8–7.8 °C temperature increase for the end of this century (IPCC, 2007; Clark and Huybers, 2009; Christensen et al., 2007).

TCD

5, 3517–3539, 2011

Eemian sea level estimates provide little constraint on the size of the GrIS, ranging from partial melting to a total loss of 7 m sea level equivalent. The highest estimates of Eemian sea level include a potentially large but unknown contribution from the Antarctic ice sheet. Due to the expansion of ice at the last glacial maximum and the erosion of potential archives, few reliable proxy data exist for Eemian ice extent except for the Greenland ice cores. The bottom sections of the summit cores (GISP2, GRIP, NGRIP) and the northwestern core at Camp Century contain Eemian ice (Dansgaard et al., 1985; Chappellaz et al., 1997; NGRIP-members, 2004), indicating that the GrIS covered these locations. The isolated ice cap on the Renland peninsula also contains ice in its bottom section, dated to be older than 130 ka (Johnsen et al., 1992). In southeastern Greenland, at the Dye-3 core site, basal ice is also found to predate the Eemian (Willerslev et al., 2007). However, due to its very old age (>400 000 yr) and the lack of direct evidence of Eemian ice, an Eemian glaciation at this site remains uncertain (Alley et al., 2010). A recent study concluded moderate melting of the southern GrIS, supporting the persistence of the southern dome and probably Dye-3 (Colville et al., 2011). Two isolated ice caps in northern and northeastern Greenland (Hans Tausen Iskappe and Flade Isblink) do not hold ice older than the thermal optimum of the present interglacial (Hammer et al., 2001; Lemark, 2010).

Previous model studies of the last interglacial find substantial melting of the southern part of the Greenland ice sheet, equivalent to a global sea level rise of 4–5.5 m (Cuffey and Marshall, 2000) or 2–3 m (Otto-Bliesner et al., 2006). The low estimate requires melting of the southern dome of the GrIS, whereas the high estimate requires additional melting of the northernmost part of the GrIS. Both studies explain a substantial part of the reconstructed sea level high stand of the last interglacial, but are not in accord with evidence for the presence of Eemian ice at the core locations discussed above.

We simulate the GrIS at 126 ka, using a three-dimensional ice sheet model, forced with a climate simulation from a comprehensive coupled climate model. In contrast to previous studies, strongest melting occurs in the northern GrIS. The robustness of this result is validated with a large ensemble simulation and theoretical considerations

TCD
5, 3517–3539, 2011
Melting of Northern Greenland during the last interglacial
A. Born and K. H. Nisancioglu

of ice sheet stability. This study is organized as follows. The ice sheet and climate models are described in Sect. 2. Section 3 presents results of the analysis, divided into the simulation of the GrIS (Sect. 3.1), quantification of ice sheet stability (Sect. 3.2) and the presentation of ensemble simulations (Sect. 3.3). Section 4 discusses and summarizes the results.

2 Model description

We use a three-dimensional, thermomechanical ice sheet model, SICOPOLIS 2.9 (Greve, 1997), forced with monthly temperature and total precipitation from the Institut Pierre Simon Laplace Coupled Model 4 (IPSL CM4) (Marti et al., 2005). Ice and bedrock topographies are initialized with modern observations (Amante and Eakins, 2009). The horizontal resolution of the ice sheet model is 10 km with 90 vertical layers. Ice dynamics are represented in the shallow-ice approximation, neglecting longitudinal stresses. This simplification is valid for ice masses that are thin compared to their lateral extent, flowing slowly over a horizontal bed. Ice shelves can not be simulated, nor can valley glaciers. For the GrIS, however, this is a valid and widely used approximation.

Climate forcing of the upper boundary is provided from simulations of the coupled model IPSL CM4. Three climate model experiments are used, forced with Eemian (126 ka), glacial inception (115 ka) and preindustrial (1850 AD, 0 ka) boundary conditions. All employ constant present day ice topography, surface conditions and preindustrial greenhouse gas concentrations. For the Eemian and the glacial inception, orbital parameters are adjusted to 126 ka values. While this generally is a good approximation for the Eemian, it is probably not realistic for the GrIS. However, the simulation compares well with existing proxy data, also in the vicinity of the GrIS (Braconnot et al., 2008; Born et al., 2010, 2011). Climate fields are interpolated bilinearly to match the horizontal resolution of the ice sheet model. Temperature fields are corrected for the coarse representation of the GrIS surface in IPSL CM4 and the evolving ice topography in SICOPOLIS, both with a fixed atmospheric lapse rate of $-6.5\,\mathrm{K\,km^{-1}}$. This corrected temperature is used to calculate melt following the positive degree day method (Reeh, 1991) and to estimate the solid fraction of total precipitation, which is used as accumulation. No further modifications are made to the climate forcing fields.

3 Results

Observations show that ice loss in Greenland is accelerating in recent years (Velicogna, 2009; van den Broeke et al., 2009), contributing considerably to the rise of eustatic sea level (Rignot et al., 2011). However, there is no justification to extrapolate recent changes of the GrIS to long-term trends (Oerlemans et al., 2006). About half of its current mass loss is due to dynamic adjustments (van den Broeke et al., 2009), related to retreating calving fronts of tidewater glaciers (Pritchard et al., 2009). These processes can not sustain their present rate of retreat for very long, and concern relatively limited volumes of ice. On the other hand, recently observed large and highly variable melt areas (Bhattacharya et al., 2009) probably eclipse smaller but sustained trends that are capable of causing a strong sea level rise in the long term. Melting alone is a questionable indicator for ice sheet stability, because moderate melting may have a large effect in regions with low accumulation and weak ice transport. In this regard, the dry northeastern sector of the GrIS is the most vulnerable region of the ice sheet (Fig. 1).

3.1 Simulation of the Greenland ice sheet

The duration of Eemian melting is not well-constrained by proxy data (e.g. Yokoyama and Esat, 2011). To estimate this duration, a transient simulation of the GrIS is carried out spanning the period 130 to 110 ka, forced with two time slice simulations of IPSL CM4 for 126 and 115 ka, respectively. The climate model data was interpolated onto the period 130 to 110 ka using June insolation at 65° N as a normalized scalar index. Linear interpolation has not been used because it yields unrealistic results for the

TCD
5, 3517–3539, 2011

extrapolation before 126 ka and after 115 ka. This does not occur with the insolation index that is maximum and minimum at 126 and 115 ka, respectively.

While a transient simulation is generally preferred for the investigation of the GrIS during the Eemian, this approach is limited by the ability to run climate models for periods longer than at most a few millennia. Due to insufficient proxy data, the ice sheet is initialized with present day ice and bedrock topographies at 130 ka. It is unclear whether this is a good starting date or if the present day shape of the ice sheet is a good approximation for that period. As the interpolated seasonal climate forcing of the transient experiment is only an approximation and not an accurate representation of Eemian climate evolution, this simulation is solely used to constrain the melt duration. For the Eemian this is estimated to be between 5000 and 7000 yr (Fig. 2).

A new simulation with climate forcing fixed to 126 ka values is used to investigate the most likely response of the GrIS. After 5000 yr, the loss of Greenland ice corresponds to a global sea level rise of 3.5 m (Fig. 3). Large regions become ice-free, most notably in the northeast and southwest. The locations of all deep ice core sites remain glaciated. After 5700 model years NEEM becomes ice-free, defining an upper limit for sea level rise of 4.2 m. Note, however, that evidence for Eemian ice at NEEM is not definitive. Ice at Dye-3 becomes thinner, but does not disappear until the end of the 10 000 yr simulation with constant 126 ka forcing.

In order to investigate the impact of Eemian climate on the GrIS mass balance independent of changes in ice topography, we compare the simulated mass balance for the Eemian (126 ka) and preindustrial climate (0 ka) for the first time step after model initialization, i.e. before changes in ice topography take place. With Eemian climate, melting increases everywhere (Fig. 4, left). However, despite lower melt rates, ice in the northeast disappears more rapidly than in other regions. This is primarily due to the very low accumulation in this region (Fig. 4, middle). Therefore, only a fraction of the melted ice is replaced by new snow and the strong positive ice-elevation feedback dominates the further development: as the ice surface melts to lower elevations, warmer air masses strongly enhance the melting.

TCD
5, 3517–3539, 2011

A. Born and K. H. Nisancioglu

3.2 Stability criterion

The vulnerability of different regions is quantified as the relative surface mass balance, the ratio of ablation to accumulation, ABL/ACC. Neglecting lateral transport of ice, changes in ice elevation $H(t)$ only depend on the balance between accumulation ACC and ablation ABL(t), where ACC is approximately constant, and $H(t)$ and ABL(t) vary in time:

$$\partial_t H(t) = \mathrm{ACC} - \mathrm{ABL}(t). \tag{1}$$

The positive ice-elevation feedback, the increased melting with lower elevations, can be simplified as

$$\mathrm{ABL}(t) = -\alpha H(t) \tag{2}$$

$$\partial_t \mathrm{ABL}(t) = -\alpha \partial_t H(t) \tag{3}$$

where α is a constant factor characterizing the elevation dependence of ablation. Combining Eqs. (1) and (3) yields:

$$\partial_t \mathrm{ABL}(t) = \alpha(\mathrm{ABL}(t) - \mathrm{ACC}), \tag{4}$$

dividing by accumulation:

$$\partial_t \left(\frac{\mathrm{ABL}(t)}{\mathrm{ACC}}\right) = \frac{\partial_t \mathrm{ABL}(t)}{\mathrm{ACC}} = \alpha \left(\frac{\mathrm{ABL}}{\mathrm{ACC}} - 1\right)$$
$$\Rightarrow \frac{\mathrm{ABL}}{\mathrm{ACC}}(t) = e^{\alpha t} + 1. \tag{5}$$

In equilibrium and without lateral ice transport, the ratio of melt to accumulation ABL/ACC must be one to hold ice elevation invariant. Following Eq. (5), an imbalance in the ABL/ACC ratio grows exponentially due to the ice-elevation feedback. This essentially reflects increased melting and thus ice loss while changes in accumulation

TCD
5, 3517–3539, 2011

A. Born and
K. H. Nisancioglu

are negligible (Fig. 4, middle). The *absolute change in relative surface mass balance* $(\mathrm{ABL}_{126\,\mathrm{ka}} - \mathrm{ABL}_{0\,\mathrm{ka}})/\mathrm{ACC}_{0\,\mathrm{ka}}$ provides a measure of stability (Fig. 4, right). Regions of ice retreat are identified by large changes, thus an unsustainable increase in melting. In particular, manifold imbalances reach far inland in the northeast due to the low accumulation. In contrast to the southwest, this affects not only marginal ice areas but also ice that is dynamically connected to the large interior body of the ice sheet.

By how much would the ice flow have to increase to counteract the imbalance in surface mass balance? In steady state, changes in ice elevation due to accumulation ACC, melting ABL and ice flow F balance to zero:

$$\partial_t H = \mathrm{ACC} - \mathrm{ABL} + F = 0 \tag{6}$$

$$\Rightarrow F = -(\mathrm{ACC} - \mathrm{ABL}) = -(\text{absolute surface mass balance}) \tag{7}$$

Thus, *relative changes in absolute surface mass balance* must be matched by equal changes in ice volume transport. Here again, the northeastern GrIS is identified as the least stable region with a required fivefold increase in ice flow (Fig. 5).

3.3 Ensemble simulations

To assess the robustness of our results, a large ensemble of experiments was run covering a wide range of parameter space, extending the methodology of Ritz et al. (1997) (Table 1). All experiments have been run for 10 000 yr in order to reach quasi-equilibrium.

As the GrIS loses mass, thinning in the northeast is faster than in the south (Fig. 6, left), consistent with the transient evolution of the original experiment and corroborating the higher vulnerability of the northeastern region. This result is reproduced with climate forcing from a 130 ka simulation of the Community Climate System Model 3 (CCSM3) (Otto-Bliesner et al., 2006) (Fig. 6, right). The coupling scheme for CCSM3 is identical to the description above, i.e. the interpolated climate fields are applied without modification.

TCD
5, 3517–3539, 2011

4 Discussion and summary

The stability of different regions of the GrIS under the climate of the last interglacial has been investigated using a three-dimensional ice sheet model, a large ensemble of sensitivity experiments and detailed analysis of the regional imbalance between accumulation and ablation. The main finding is that the most vulnerable region in a warm climate such as the last interglacial is northern Greenland because its dry climate with low accumulation can not compensate increased melting. This general finding is applicable to modern climate change.

Previous model studies of the Eemian identified the southern GrIS as the most vulnerable (Cuffey and Marshall, 2000; Lhomme et al., 2005; Otto-Bliesner et al., 2006). Considerable melting of the northeastern GrIS, however, has also been found in several recent simulations (Tarasov and Peltier, 2003; Robinson et al., 2011; Fyke et al., 2011). Biases of the simulated climate, especially at high northern latitudes and at the high elevations of the Greenland ice sheet, are potentially large and might explain some discrepancies between different studies. The main finding of the present study, however, is unlikely to be the result of model biases. The results have been reproduced with climate forcing of a second comprehensive climate model. Both climate models have been validated to simulate Eemian climate consistent with proxy data in previous studies (Overpeck et al., 2006; Otto-Bliesner et al., 2006; Braconnot et al., 2008; Born et al., 2010, 2011). The impact of contingent climate biases is effectively simulated by changing the melt parameters of the ice sheet model, which was found to not change the high vulnerability of the northeastern GrIS. Similarly, the wide range of parameters changing the ice sheet dynamics makes a dependence on the choice of ice sheet model unlikely as well.

Currently available proxy data is inconclusive on the shape of the Eemian GrIS. Pollen in marine sediments off the south Greenland coast has been interpreted to imply considerable melting of the GrIS to allow for growth of extensive vegetation (de Vernal and Hillaire-Marcel, 2008). Considerable melting of the GrIS in the south is supported

TCD
5, 3517–3539, 2011
Melting of Northern Greenland during the last interglacial
A. Born and K. H. Nisancioglu

by the finding of a greater discharge of glacial flour during the last interglacial than during the early Holocene (Carlson et al., 2008). However, isotopic analysis of the glacial flour off Greenland has recently been found to source from all 3 south Greenland Precambrian terranes and thus significant ice remained on southern Greenland through the Eemian (Colville et al., 2011). An early analysis of basal ice from Dye-3 concluded that ice at this location disappeared during the Eemian, as well as at Camp Century (Koerner, 1989). However, several melt layers have been found in the bottom section of Dye-3, which document a warm period with persistent ice during the last interglacial (Dansgaard et al., 1985; Souchez et al., 1998). This has been confirmed by advanced dating techniques providing direct evidence of ice predating the Eemian (Willerslev et al., 2007).

Note however, that the existence of ice at Dye-3 and in southern Greenland during the last interglacial does not preclude a considerable sea level contribution from other sectors of the Greenland ice sheet. Unfortunately there are no deep ice cores in northeastern Greenland. However, there are widespread marine deposits in this area from the last interglacial, particularly during the period of peak warmth (~123 ka; Funder, 1989; Mangerud and Funder, 1994; Alley et al., 2010). This indicates that seawater was present far inland following the penultimate glacial period, consistent with our model results. Marine conditions in northeastern Greenland did not end until late in the last glacial cycle (Houmark-Nielsen et al., 1994), suggesting that the ice margin retreated considerably during the Eemian.

Eemian ice was also found in the isolated ice cap on the Renland peninsula in eastern Greenland (Johnsen et al., 1992). A 20 % increase in precipitation was reconstructed for the lowest 5 m of ice, as well as numerous melt layers. This is consistent with our interpretation that ice persisted due to high accumulation and despite the warmer climate and increased melting.

An estimate on the contribution of ice sheets to sea level rise is one of the most pressing needs for the assessment of future climate change (IPCC, 2007). The identification of key regions is a necessary requirement for which the Eemian, despite a

TCD
5, 3517–3539, 2011

different cause of warming, holds valuable information. A comparison of latitudinal sea surface and air temperature gradients based on proxy data from the last interglacial with the projected greenhouse warming for the twenty-first century show a striking fit (Clark and Huybers, 2009), suggesting that the Greenland ice sheet might once again experience a sustained period with temperatures comparable to that of the last interglacial, with its potential consequences for global sea level. Recent trends in ablation, however, must be interpreted with caution. Wake et al. (2009) show that negative surface mass balance anomalies in Greenland between 1995 and 2005 are not unprecedented in the last 140 yr, thus at least partly representing natural variability. A notable exception is the northeastern part of the GrIS, indicating that the recent increase in melting in this region might be a long-term trend. High current rates of mass loss in northeastern Greenland are also evident from detailed mass budget calculations (van den Broeke et al., 2009) and gravimetry (Chen et al., 2006; Ramillien et al., 2006). A warmer climate over southern Greenland does not necessarily entail the disappearance of the southern dome as is demonstrated in this study of the Eemian interglacial.

Acknowledgements. We gratefully acknowledge Ralf Greve for public availability and comprehensive documentation of SICOPOLIS, Pascale Braconnot for providing data of IPSL CM4 as well as Bette Otto-Bliesner for data of CCSM3. Our work greatly benefited from discussions with Sigfús J. Johnsen and Bette L. Otto-Bliesner, and a through review of an early version of the manuscript by Shawn J. Marshall. ERA-40 data used in this study have been provided by the European Centre for Medium-Range Weather Forecasts. Greenland melt data based on passive microwave radiation was provided by the US National Snow and Ice Data Center. Computer time was provided by the Research Council of Norway through the NOTUR project. A. B. received support from the Marie Curie project NICE (MRTN-CT-2006-036127) and the Swiss National Centre for Competence in Research "Climate". This is publication no. 384 from the Bjerknes Centre for Climate Research.

TCD
5, 3517–3539, 2011

Melting of Northern Greenland during the last interglacial

A. Born and K. H. Nisancioglu

References

Abdalati, W.: Greenland Ice Sheet Melt Characteristics Derived from Passive Microwave Data, Tech. rep., National Snow and Ice Data Center, Boulder, Colorado USA, 2007. 3534

Alley, R., Andrews, J., Brigham-Grette, J., Clarke, G., Cuffey, K., Fitzpatrick, J., Funder, S., Marshall, S., Miller, G., Mitrovica, J., Muhs, D. R., Otto-Bliesner, B., Polyak,L., and White, J.: History of the Greenland Ice Sheet: paleoclimatic insights, Quaternary Sc. Rev., 29, 1728–1756, 2010. 3519, 3526

Amante, C. and Eakins, B. W.: ETOPO1 1 Arc-Minute Global Relief Model: Procedures, Data Sources and Analysis, Tech. rep., NOAA Technical Memorandum NESDIS NGDC-24, 2009. 3520

Bhattacharya, I., Jezek, K. C., Wang, L., and Liu, H.: Surface melt area variability of the Greenland ice sheet: 1979–2008, Geophysi. Res. Lett., 36, L20502, doi:10.1029/2009GL039798, 2009. 3521

Born, A., Nisancioglu, K. H., and Braconnot, P.: Sea ice induced changes in ocean circulation during the Eemian, Clim. Dynam., 35, 1361, doi:10.1007/s00382-009-0709-2, 2010. 3520, 3525

Born, A., Nisancioglu, K. H., and Risebrobakken, B.: Late Eemian warming in the Nordic Seas as seen in proxy data and climate models, Paleoceanography, 26, PA2207, doi:10.1029/2010PA002027, 2011. 3520, 3525

Braconnot, P., Marzin, C., Grégoire, L., Mosquet, E., and Marti, O.: Monsoon response to changes in Earth's orbital parameters: comparisons between simulations of the Eemian and of the Holocene, Clim. Past, 4, 281–294, doi:10.5194/cp-4-281-2008, 2008. 3520, 3525

CAPE members: Last Interglacial Arctic warmth confirms polar amplification of climate change, Quaternary Sci. Rev., 25, 1383–1400, doi:10.1016/j.quascirev.2006.01.033, 2006. 3518

Carlson, A., Stoner, J., Donnelly, J., and Hillaire-Marcel, C.: Response of the southern Greenland Ice Sheet during the last two deglaciations, Geology, 36, 359–362, 2008. 3526

Chappellaz, J., Brook, E., Blunier, T., and Malaizé, B.: CH_4 and $\delta^{18}O$ of O_2 records from Antarctic and Greenland ice: A clue for stratigraphic disturbance in the bottom part of the Greenland Ice Core Project and the Greenland Ice Sheet Project 2 ice cores, J. Geophys. Res., 102, 26547–26557, doi:10.1029/97JC00164, 1997. 3519

Chen, J. L., Wilson, C. R., and Tapley, B. D.: Satellite gravity measurements confirm accelerated melting of Greenland ice sheet, Science, 313, 1958–1960, 2006. 3527

Christensen, J., Hewitson, B., Busuioc, A., Chen, A., Gao, X., Held, I., Jones, R., Kolli, R., Kwon, W.-T., Laprise, R., Magaña Rueda, V., Mearns, L., Menéndez, C., Räisänen, J., Rinke, A., Sarr, A., and Whetton, P.: Regional Climate Projections, in: Climate Change 2007: The Physical Science Basis. Contribution of Working Group I to the Fourth Assessment Report of the Intergovernmental Panel on Climate Change, edited by: Solomon, S., Qin, D., Manning, M., Chen, Z., Marquis, M., Averyt, K. B., Tignor, M., and Miller, H. L., Cambridge University Press, Cambridge, United Kingdom and New York, NY, USA, 2007. 3518

Clark, P. U. and Huybers, P.: Interglacial and future sea level, Nature, 462, 856–857, 2009. 3518, 3527

Colville, E. J., Carlson, A. E., Beard, B. L., Hatfield, R. G., Stoner, J. S., Reyes, A. V., and Ullman, D. J.: Sr-Nd-Pb Isotope Evidence for Ice-Sheet Presence on Southern Greenland During the Last Interglacial, Science, 333, 620–623, doi:10.1126/science.1204673, 2011. 3519, 3526

Cuffey, K. and Marshall, S.: Substantial contribution to sea level rise during the last interglacial from the Greenland Ice Sheet, Nature, 404, 591–594, 2000. 3519, 3525

Dansgaard, W., Clausen, H., Gundestrup, N., Johnsen, S., and Rygner, C.: Dating and climatic interpretation of two deep greenland ice cores, in: Greenland Ice Core: Geophysics, Geochemistry, and the Environment, edited by: Langway, C. C., Oeschger, H., and Dansgaard, W., AGU Geophysical Monograph Series no. 33, Washington, DC, 71–76, 1985. 3519, 3526

de Vernal, A. and Hillaire-Marcel, C.: Nature Variability of Greenland Climate Vegetation, and Ice Volume During the Past Million Years, Science, 320, 1622–1625, 2008. 3525

Funder, S.: Quaternary geology of the ice-free areas and adjacent shelves of Greenland, in: Quaternary Geology of Canada and Greenland, edited by: Fulton, R. J., Geological Survey of Canada, Geology of Canada, 739–792, 1989. 3526

Fyke, J. G., Weaver, A. J., Pollard, D., Eby, M., Carter, L., and Mackintosh, A.: A new coupled ice sheet/climate model: description and sensitivity to model physics under Eemian, Last Glacial Maximum, late Holocene and modern climate conditions, Geosci. Model Dev., 4, 117–136, doi:10.5194/gmd-4-117-2011, 2011. 3525

Greve, R.: A continuum-mechanical formulation for shallow polythermal ice sheets, Philos. T. R. Soc. Lond., 355, 921–974, 1997. 3520

Hammer, C., Johnsen, S., Clausen, H., Dahl-Jensen, D., Gundestrup, N., and Steffensen, J.: The Paleoclimatic Record from a 345 m long Ice Core from the Hans Tausen Iskappe, Meddelelser om Grønland, Geoscience, 39, 87–95, 2001. 3519

Houmark-Nielsen, M., Hansen, L., Jørgensen, M. E., and Kronborg, C.: Stratigraphy of a Late Pleistocene ice-cored moraine at Kap Herschell, Northeast Greenland, Boreas, 23, 505–512, doi:10.1111/j.1502-3885.1994.tb00618.x, 1994. 3526

IPCC: Climate Change 2007: The Physical Science Basis. Contribution of Working Group I to the Fourth Assessment Report of the Intergovernmental Panel on Climate Change, edited by: Solomon, S., Qin, D., Manning, M., Chen, Z., Marquis, M., Averyt, K. B., Tignor, M., and Miller, H. L., Cambridge University Press, Cambridge, United Kingdom and New York, NY, USA, 2007. 3518, 3526

Jansen, E., Overpeck, J., Briffa, K., Duplessy, J.-C., Joos, F., Masson-Delmotte, V., Olago, D., Otto-Bliesner, B., Peltier, W., Rahmstorf, S., Ramesh, R., Raynaud, D., Rind, D., Solomina, O., Villalba, R., and Zhang, D.: Palaeoclimate, in: Climate Change 2007: The Physical Science Basis. Contribution of Working Group I to the Fourth Assessment Report of the Intergovernmental Panel on Climate Change, edited by: Solomon, S., Qin, D., Manning, M., Chen, Z., Marquis, M., Averyt, K. B., Tignor, M., and Miller, H. L., Cambridge University Press, Cambridge, United Kingdom and New York, NY, USA, 2007. 3518

Johnsen, S. J., Clausen, H. B., Dansgaard, W., Gundestrup, N. S., Hansson, M., Jonsson, P., Steffensen, J. P., and Sveinbjørnsdottir, A. E.: A “deep” ice core from East Greenland, Meddelelser om Grønland, Geoscience, 29, 3–22, 1992. 3519, 3526

Koerner, R. M.: Ice Core Evidence for Extensive Melting of the Greenland Ice Sheet in the Last Interglacial, Science, 244, 964–968, doi:10.1126/science.244.4907.964, 1989. 3526

Kopp, R. E., Simons, F. J., Mitrovica, J. X., Maloof, A. C., and Oppenheimer, M.: Probabilistic assessment of sea level during the last interglacial stage, Nature, 467, 863–868, doi:10.1038/nature08686, 2009. 3518

Lemark, A.: A study of the Flade Isblink ice cap using a simple ice flow model, Master’s thesis, Niels Bohr Institute, Copenhagen University, 2010. 3519

Lhomme, N., Clarke, G. K. C., and Marshall, S. J.: Tracer transport in the Greenland Ice Sheet: constraints on ice cores and glacial history, Quaternary Sci. Rev., 24, 173–194, 2005. 3525

Loutre, M.-F., Paillard, D., Vimeux, F., and Cortijo, E.: Does mean annual insolation have the potential to change the climate?, Earth Planet. Sc. Lett., 221, 1–14, 2004. 3518

Mangerud, J. and Funder, S.: The interglacial-glacial record at the mouth of Scoresby Sund, East Greenland, Boreas, 23, 349–358, 1994. 3526

Marti, O., Braconnot, P., Bellier, J., Benshila, R., Bony, S., Brockmann, P., Cadule, P., Caubel, A., Denvil, S., Dufresne, J.-L., Fairhead, L., Filiberti, M.-A., Foujols, M.-A., Fichefet, T., Friedlingstein, P., Gosse, H., Grandpeix, J.-Y., Hourdin, F., Krinner, G., Lévy, C., Madec, G., Musat, I., de Noblet, N., Polcher, J., and Talandier, C.: The new IPSL climate system model: IPSL-CM4, Tech. rep., IPSL Global Climate Modeling Group, 2005. 3520

NGRIP-members: High-resolution record of Norhtern Hemisphere climate extending into the last interglacial period, Nature, 431, 147–151, 2004. 3519

Oerlemans, J., Dahl-Jensen, D., and Masson-Delmotte, V.: Ice sheets and sea level, Science, 313, 1043–1045, 2006. 3521

Otto-Bliesner, B. L., Marshall, S. J., Overpeck, J. T., Miller, G. H., Hu, A., and CAPE Last Interglacial Project members: Simulating Arctic Climate Warmth and Icefield Retreat in the Last Interglaciation, Science, 311, 1751–1753, 2006. 3518, 3519, 3524, 3525

Overpeck, J. T., Otto-Bliesner, B. L., Miller, G. H., Muhs, D. R., Alley, R. B., and Kiehl, J. T.: Paleoclimatic Evidence for Future Ice-Sheet Instability and Rapid Sea-Level Rise, Science, 311, 1747–1750, 2006. 3518, 3525

Petit, J. R., Jouzel, J., Raynaud, D., Barkov, N. I., Barnola, J.-M., Basile, I., Bender, M., Chappellaz, J., Davisk, M., Delaygue, G., Delmotte, M., Kotlyakov, V. M., Legrand, M., Lipenkov, V. Y., Lorius, C., Pin, L. P., Ritz, C., Saltzmank, E., and Stievenard, M.: Climate and atmospheric history of the past 420,000 years from the Vostok ice core, Antarctica, Nature, 399, 429–436, 1999. 3518

Pritchard, H. D., Arthern, R. J., Vaughan, D. G., and Edwards, L. A.: Extensive dynamic thinning on the margins of the Greenland and Antarctic ice sheets, Nature, 461, 971–975, doi:10.1038/nature08471, 2009. 3521

Ramillien, G., Lombard, A., Cazenave, A., Ivins, E., Llubes, M., Remy, F., and Biancale, R.: Interannual variations of the mass balance of the Antarctica and Greenland ice sheets from GRACE, Global Planet. Change, 53, 198–208, doi:10.1016/j.gloplacha.2006.06.003, 2006. 3527

Reeh, N.: Parameterization of melt rate and surface temperature on the Greenland Ice Sheet, Polarforschung, 59, 113–128, 1991. 3521

Rignot, E., Velicogna, I., van den Broeke, M. R., Monaghan, A., and Lenaerts, J.: Acceleration of the contribution of the Greenland and Antarctic ice sheets to sea level rise, Geophys. Res. Lett., 38, L05503, doi:10.1029/2011GL046583, 2011. 3521

Ritz, C., Fabre, A., and Letréguilly, A.: Sensitivity of a Greenland ice sheet model to ice flow and ablation parameters: consequences for the evolution through the last climatic cycle, Clim. Dynam., 13, 11–24, 1997. 3524

Robinson, A., Calov, R., and Ganopolski, A.: Greenland ice sheet model parameters constrained using simulations of the Eemian Interglacial, Clim. Past, 7, 381–396, doi:10.5194/cp-7-381-2011, 2011. 3525

Souchez, R., Bouzette, A., Clausen, H., Johnsen, S., and Jouzel, J.: A stacked mixing sequence at the base of the Dye 3 core, Greenland, Geophys. Res. Lett., 25, 1943–1946, 1998. 3526

Tarasov, L. and Peltier, W. R.: Greenland glacial history, borehole constraints, and Eemian extend, J. Geophys. Res., 108, 2143, doi:10.1029/2001JB001731, 2003. 3525

van den Broeke, M., Bamber, J., Ettema, J., Rignot, E., Schrama, E., van de Berg, W. J., van Meijgaard, E., Velicogna, I., and Wouters, B.: Partitioning Recent Greenland Mass Loss, Science, 326, 984–986, 2009. 3521, 3527

Velicogna, I.: Increasing rates of ice mass loss from the Greenland and Antarctic ice sheets revealed by GRACE, Geophys. Res. Lett., 36, L19503, doi:10.1029/2009GL040222, 2009. 3521

Wake, L., Huybrechts, P., Box, J., Hanna, E., Janssens, I., and Milne, G.: Surface mass-balance changes of the Greenland ice sheet since 1866, Ann. Glaciol., 50, 178–184, 2009. 3527

Willerslev, E., Cappellini, E., Boomsma, W., Nielsen, R., Hebsgaard, M. B., Brand, T. B., Hofreiter, M., Bunce, M., Poinar, H. N., Dahl-Jensen, D., Johnsen, S., Steffensen, J. P., Bennike, O., Schwenninger, J.-L., Nathan, R., Armitage, S., de Hoog, C.-J., Alfimov, V., Christl, M., Beer, J., Muscheler, R., Barker, J., Sharp, M., Penkman, K. E., Haile, J., Taberlet, P., Thomas, M., Gilbert, P., Casoli, A., Campani, E., and Collins, M. J.: Ancient Biomolecules from Deep Ice Cores Reveal a Forested Southern Greenland, Science, 317, 111–114, 2007. 3519, 3526

Yokoyama, Y. and Esat, T.: Global climate and sea level: Enduring variability and rapid fluctuations over the past 150,000 years, Oceanography, 24, 54–69, doi:10.5670/oceanog.2011.27, 2011. 3521

TCD

5, 3517–3539, 2011

Table 1. Parameter range for ensemble experiments and standard values used in the simulations. Heat flux is non-uniform in the standard experiment. One experiment for every possible permutation of the above parameters has been carried out, for two different climate forcings, giving a total of 5184 model simulations (see Fig. 6).

parameter	value	standard value	unit
geothermal heat flux	30..10..80	$\sim$65	$\mathrm{mW\,m^{-2}}$
degree-day factor for snow	3..8	5	$\mathrm{mm\,day^{-1}\,K^{-1}}$
degree-day factor for ice	10..2..20	14	$\mathrm{mm\,day^{-1}\,K^{-1}}$
basal sliding	5..2..15	11.2	$\mathrm{m\,a^{-1}\,Pa^{-1}}$
flow enhancement factor	1, 3	3	dimensionless

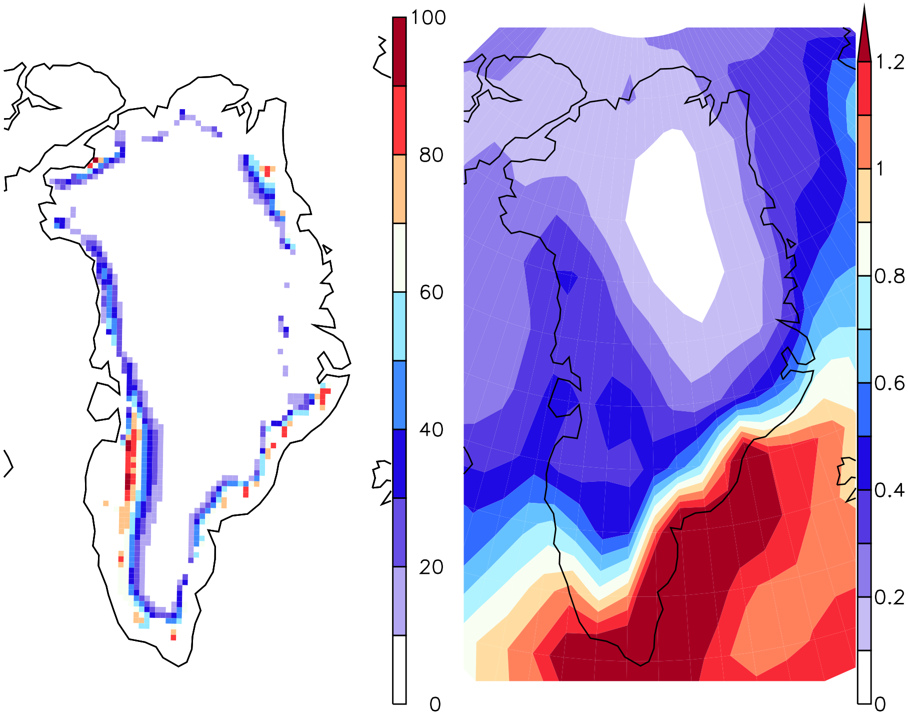

Fig. 1. Observed average duration of melt season in 1979–2007 (left, in days) (Abdalati, 2007), and average total precipitation in 1958–2001 from ERA-40 (right, in m yr^{-1}). As in the south, the northeastern region of the ice sheet shows a long melt season. Unlike regions in the south, however, the northeast receives very little precipitation to balance the melting.

TCD
5, 3517–3539, 2011

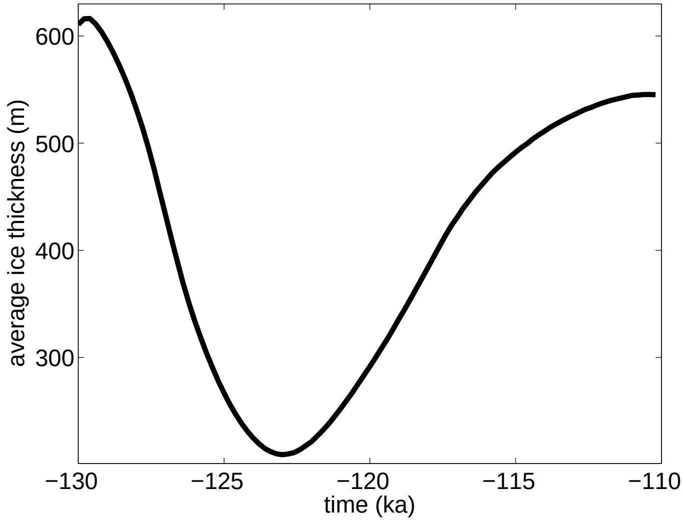

Fig. 2. Average ice thickness evolution of the GrIS between 130 and 110 ka. The model was initialized with preindustrial ice and bedrock topographies. Some adjustment is visible in the first 1000 yr. After that, ice melts for 5000 to 7000 yr, followed by a recovery at the end of the last interglacial.

TCD
5, 3517–3539, 2011

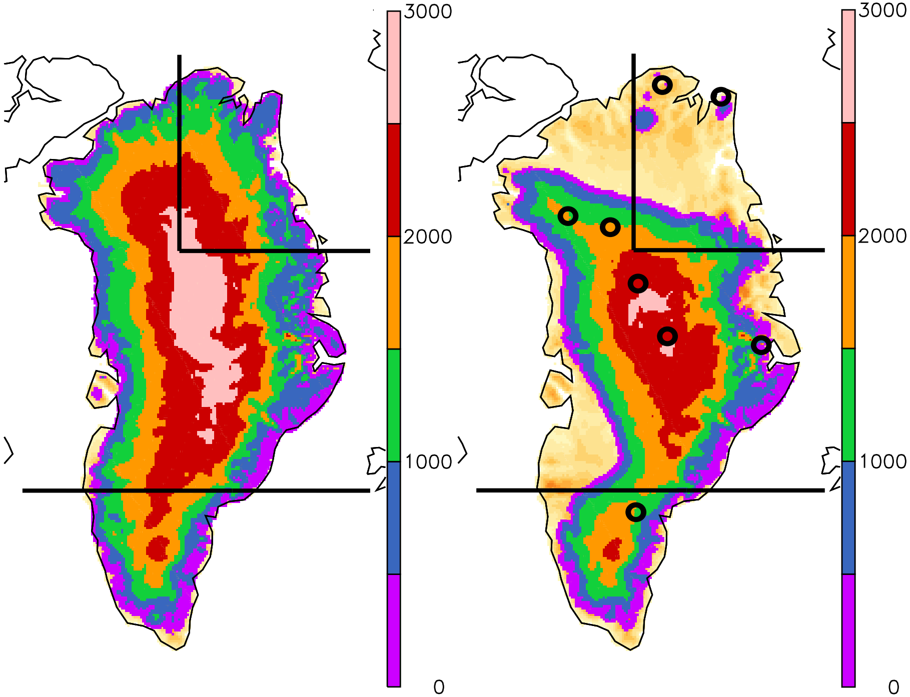

Fig. 3. Modelled ice thickness (in m) for present day (left) and 126 ka (right), after 5000 yr of simulation. Regions defined for this study are separated by bold black lines. Circles show locations of ice core sites (from north to south: Hans Tausen Iskappe, Flade Isblink, Camp Century, NEEM, NGRIP, GRIP, Renland, Dye-3). Preindustrial ice area and thickness are well reproduced. With 126 ka forcing, the Greenland ice sheet melts mostly from the northeast and southwest. The southern dome does not disappear.

TCD
5, 3517–3539, 2011

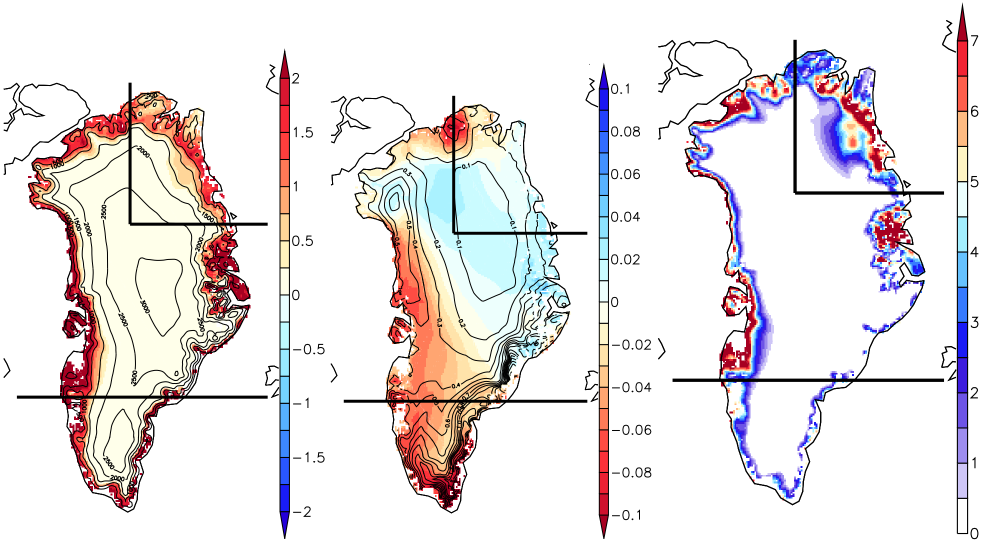

Fig. 4. Anomalies and ratios of change at the first model time step, thus independent from changes in ice topography and dynamics: left: melt anomaly "126–0 ka" (color, $\mathrm{m\,yr^{-1}}$) and initial ice elevation (contours, m). Middle: accumulation anomaly "126–0 ka" (color, $\mathrm{m\,yr^{-1}}$) and total accumulation at 0 ka (contours, $\mathrm{m\,yr^{-1}}$). Right: ratio between melt anomaly and preindustrial accumulation, $(ABL_{126\,ka} - ABL_{0\,ka})/ACC_{0\,ka}$, as a measure of instability. Values greater than 1 increase exponentially if not balanced by ice flow. With 126 ka climate boundary conditions, melting increases throughout the entire ice sheet, mostly in low-lying regions and in large regions in northern Greenland. Accumulation of snow is reduced in the south and west of the ice sheet due to higher temperatures. Also as a result of higher atmospheric temperatures and vapor content, especially at higher altitudes, accumulation slightly increases in central and north-eastern Greenland, but approximately two orders of magnitude less than the increase in melting. The northeastern region of Greenland is the least stable as quantified by relative changes in surface mass balance.

TCD

5, 3517–3539, 2011

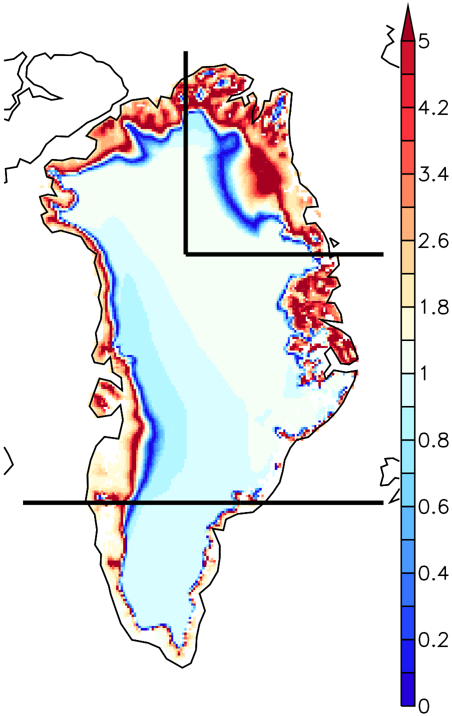

Fig. 5. Ratio of absolute surface mass balances, $(\text{ACC-ABL})_{126\,\text{ka}}/(\text{ACC-ABL})_{0\,\text{ka}}$. For mass flow to balance surface imbalances, it needs to increase by the same factor. The northeastern GrIS is identified as the least stable region. The required fivefold increase in ice flux over a large region is unrealistic. In contrast, the region of manifold surface mass balance in the southwest is a relatively thin band restricted to the margin. Steep surface slopes are already present and further enhanced by melting of the lowest elevation ice. This dynamical regime is different from the northeast and ice flow can effectively slow down ice loss. Moreover, where there is melting in the west, the ice divide moves east, thereby drawing more ice from the stable region to the southeast of the ice sheet which receives most accumulation.

TCD
5, 3517–3539, 2011

Melting of Northern Greenland during the last interglacial

A. Born and
K. H. Nisancioglu

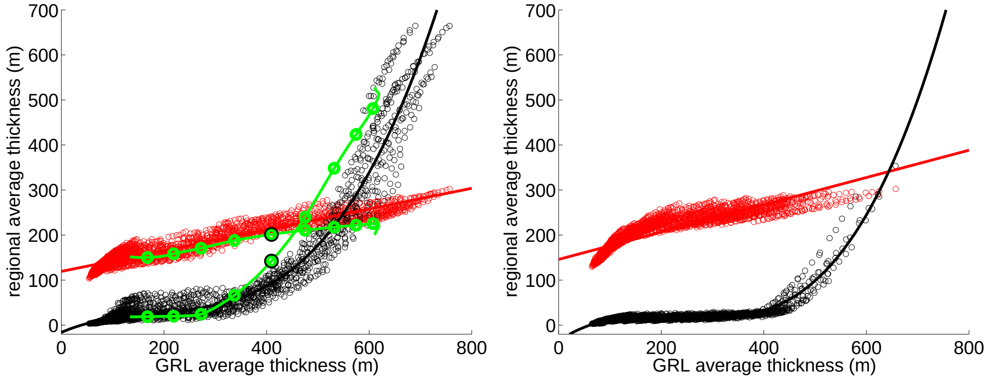

Fig. 6. Simulated average ice thickness in northeastern (black) and and southern (red) regions, as a function of the average ice thickness of the entire ice sheet, for 126 ka in IPSL CM4 (left) and 130 ka in CCSM3 (right). Each data point corresponds to one of 5184 ensemble members with a different set of parameters, run for 10 000 yr. Polynomial fits of first and third order are included for visibility. The transient evolution of the simulation of Fig. 3 is shown in green with circles spaced every 1000 yr. Ice thickness in northeastern Greenland responds rapidly to a reduction in total ice thickness, while ice in southern Greenland is more stable. This result is independent of the simulated climate.

TCD
5, 3517–3539, 2011

A. Born and K. H. Nisancioglu